Tilting and twirling as myosin V steps along actin filaments as detected by fluorescence polarization

David M. Warshaw

Department of Molecular Physiology and Biophysics, University of Vermont, Burlington, VT 05405

The Journal of General Physiology

The myosin superfamily of mechanoenzymes, more commonly referred to as molecular motors, converts chemical energy from the hydrolysis of ATP into mechanical work through its cyclic interactions with actin, which serves as a cytoskeletal track for myosin. Various classes of myosin perform such basic cellular processes that range from muscle contraction to intracellular cargo transport and exocytosis. Class V myosins (myoV) are one of the most highly studied processive molecular motors, which have the ability to travel long distances (>1 µm) by taking multiple, 36-nm hand-over-hand steps without falling off their actin tracks (Forkey et al., 2003; Warshaw et al., 2005). This ability makes the motor well suited for directed intracellular cargo transport along the actin cytoskeleton, traveling from the cell center toward the cell periphery. However, the intracellular actin highway is extremely complex, consisting of a 3-D meshwork of intersecting actin filaments and cross-linked filaments (i.e., bundles) that present a physical challenge to efficient myoV transport. How myoV copes with these cytoskeletal challenges requires an understanding of how this molecular motor's structure allows it to be adept at maneuvering through the cell's actin meshwork. In this issue, Lewis et al. paint an elegant 3-D picture of how myoV motors engage their actin track using state-of-the-art single-molecule fluorescence microscopy, providing molecular structure and function in real time as the myoV molecule walks step by step in vitro along a single actin filament adhered to a glass microscope slide (Figs. 1 and 2). By placing rigidly coupled fluorescent probes at specific locations on the myoV motor (Fig. 1), fluorescence polarization (pol) measurements in a total internal reflectance fluorescence (TIRF) microscope provided high temporal (80 ms) and angular (10°) resolution, polTIRF readouts of the myoV's conformational orientation relative to its actin track for each step taken by the motor. Knowing the limits of myoV's structural flexibility and how it contributes to its processive motion in vitro are critical pieces of information that must be defined before appreciating how in vivo myoV deals with the complexity of the actin cytoskeleton.

MyoV, which shares many structural attributes with other members of the myosin superfamily (Fig. 1), is composed of two heavy chains, each having four distinct structural domains described as follows: (1) an N-terminal globular head that has both an actin-binding site and a catalytic site for ATP hydrolysis; (2) emanating from each head is a long neck, containing six IQ domains that bind calmodulin and rigidify the neck so that it can act as a lever arm to amplify small conformations in the head associated with the hydrolysis of ATP; (3) following the lever arm is an α-helical coiled-coil dimerization domain so that the motor becomes effectively two-headed; and, finally, (4) a C-terminal globular tail domain for cargo binding and regulation/inhibition of the motor's activity. In the study by Lewis et al. (2012), two expressed myoV constructs were generated, one having its normal 6IQ lever and the other having a shorter 4IQ lever (Fig. 1). Both constructs were devoid of the globular tail domain, making these motors constitutively active.

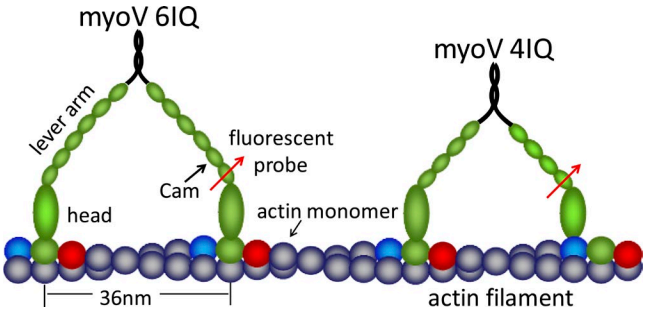

Figure 1. myoV and actin structure. myoV, a double-headed molecular motor, is composed of a lever arm that has calmodulin (Cam) bound to six IQ domains. For fluorescence polarization measurements, a fluorescent probe (red arrow) is bound to one of the Cams. A short myoV 4IQ construct was also expressed. The actin filament track is composed of individual actin monomers, with the preferable binding site for the myoV 6IQ heads highlighted in green. Occasionally, the motor steps one monomer short (blue) or long (red) of the preferable site.

Correspondence to David M. Warshaw: david.warshaw@uvm.edu

The Rockefeller University Press
J. Gen. Physiol. Vol. 139 No. 2 97–100
www.jgp.org/cgi/doi/10.1085/jgp.201210769

MyoV's processive walking behavior is brought about by an exquisite coordination of its two heads, one of which leads while the other trails (Fig. 2 A). For a forward step to occur, the trailing head must first detach after the release of the hydrolysis product (ADP) and rebinding of ATP, while at the same time the leading head must complete its powerstroke, swinging its lever arm and thrusting the trailing head forward so that it binds to the actin filament to become the new leading head (Fig. 2 A). For the motor to have a forward stepping bias and thus limit the probability of taking a backward step or detaching from actin prematurely, the enzymatic cycles for the two heads are gated (Veigel et al., 2002) as a result of intramolecular communication. This cross talk between heads results from the strain set up by the leading head attempting to undergo its powerstroke before the trailing head detaches. This intramolecular strain accelerates the detachment of the trailing head while slowing the detachment of the leading head, thus guaranteeing that the trailing head detaches first and that one head remains attached to the actin track, ensuring processive forward motion without the motor terminating its run. With the myoV lever arms having such well-defined orientations during the period that both heads are attached to actin (Figs. 1 and 2), it is not surprising that the motor lends itself to structural characterization through the use of single-molecule polTIRF measurements. In fact, if the motor walks in a hand-over-hand fashion as described above, fluorescent probes placed at known locations on the lever arm should alternate between two defined orientations as each head alternates between leading and trailing head. To observe this phenomenon in real time, Lewis et al. (2012) exchanged one of the calmodulins on the lever with an expressed calmodulin having two cysteines for attachment of a bifunctional rhodamine probe (Fig. 1). Although the experiment sounds simple, the analysis of the results is far more complex. For example, the orientation of the probe on the lever arm is highly variable depending which calmodulin is exchanged, although more often than not it is the three calmodulins closest to the head that are exchanged (Fig. 1). Second, how the actin adheres to the glass slide is variable. Even more complex is the motor's ability to bind at different locations along the actin filament, which adds further ambiguity to how the probe orientation relates to the orientation of the lever arm relative to the actin filament's frame of reference. Although the motor's capacity to bind to different sites on actin may introduce unwanted analytical complications, this critically important property allows it to maneuver through the complex actin cytoskeleton. Lewis et al. (2012) succeeded in developing a rigorous analytical solution to estimating the probe orientation so as to provide the most direct measure of both the lever arms axial (in the plane along the actin filament's long axis) and azimuthal (in a plane perpendicular to the actin filament's long axis) angles relative to the actin filament (Fig. 2).

Through a series of geometrical transformations, Lewis et al. (2012) determine the lever-arm angle on a step-by-step basis and as previously concluded by Forkey et al. (2003) from just the fluorescent probe angles, the lever arm alternates between axial angles, β, of 120° and 60° for the leading and trailing lever arms, respectively (Fig. 2 A). These are in remarkable agreement with lever-arm conformations observed in electron microscopic (EM) images in which the myoV molecule is captured while paused on actin with both heads firmly bound to the filament (Walker et al., 2000). Where the investigators in the present study go beyond their previously published work (Forkey et al., 2003) is through the use of their detailed geometrical analysis of the fluorescent probe's local angular orientation to transform this spatial information into the 3-D orientation of the myoV lever arm relative to actin as the motor occasionally binds either one actin monomer short of or one monomer beyond that which it would prefer to step on (Fig. 2). To understand this, one must appreciate the structure of the actin filament and the structural limitations that it places on myosin's stereospecific binding to actin.

Actin filaments result from the polymerization of actin monomers into two strands that form a right-handed helix with the half-repeat occurring every 13 monomers (total number of monomers for both strands) or 36 nm (Figs. 1 and 2). With every monomer a potential binding site for myosin, it is not surprising that the structure of the normal 6IQ myoV allows it to span this 36-nm repeat and thus walk along the ridge of the actin filament by stepping on every 13th actin monomer (Fig. 2 A). However, the potential for myoV to step shorter (Fig. 2 B) or longer (Fig. 2 C) than this optimum 13th monomer-binding site on actin was first observed in EM images (Walker et al., 2000) and from studies in which myoV while walking on an actin filament "tightrope" appeared to walk along a spiral path that describes a left-handed helix with a pitch of 2.2 µm (Ali et al., 2002). For this to have occurred, the myoV motor must have stepped occasionally on the 11th monomer and in doing so biased the motor's trajectory along a spiral track that reflects the helical nature of the actin filament. Because myosin binds actin stereospecifically, binding of the leading head to the 11th monomer requires the motor's lever arm to adopt an off-axis angular (i.e., azimuthal, α) orientation (Fig. 2 B). In fact, given the actin filament structure, each actin monomer's myoV-binding site is offset from its neighboring monomer within the strand by ∼28°, which should force the orientation of the myoV head and lever to conform to this structural constraint. This potential azimuthal orientation of the lever was confirmed by Lewis et al. (2012) by calculating the difference in the azimuthal angle ($\Delta\alpha$) of the leading

head between two successive steps. If the leading head landed only on the 13th monomer, the lever's azimuthal angle would always be the same and this would result in the $\Delta\alpha$ being zero degrees between successive steps of the head (Fig. 2 A). However, if the leading head landed one monomer short or long of the optimum, the expected absolute $\Delta\alpha$ would be $\sim$28°, which in fact it was (Fig. 2 B). Interestingly, the majority of the time (55%) the myoV stepped faithfully on the 13th monomer, but 25% of the time it stepped one monomer short, and 20% of the time it stepped one monomer long. These data provide strong evidence that the slight bias toward occasionally stepping on the 11th actin monomer will force the motor to take a left-handed spiral path along the actin filament, as reported in the actin tight-rope experiments (Ali et al., 2002). This was further confirmed by Lewis et al. (2012) in an inverted assay where the myoV motors were adhered to the microscope slide and the actin filaments, which were propelled by the myoV, appeared to twirl, predominantly in a left-handed manner. This was determined using the same polTIRF setup to characterize the change in orientation of rhodamine probes that were used to sparsely label actin filaments.

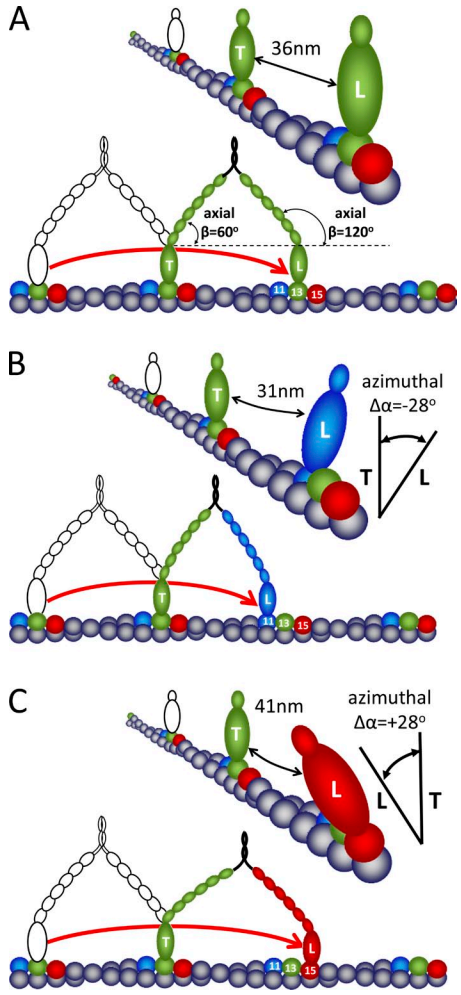

Figure 2. myoV stepping and head orientation. (A) The motor steps in a hand-over-hand manner (red arrow), where the initial position is in white and the motor's subsequent position is in color. The trailing (T) and leading (L) heads bind 36 nm apart, being preferentially bound to the 13th actin monomer (green). The axial angles adopted by the two heads are indicated. The top section highlights the head orientation. (B) Same as A, except that the leading head lands one monomer short (11th in blue) of the preferred site (13th in green), resulting in the heads being 31 nm apart and offset azimuthally by −28°. (C) Same as A, except that the leading head lands one monomer long (15th in red) of the preferred site (13th in green), resulting in the heads being 41 nm apart and offset azimuthally by +28°.

Another twist to the story was the characterization of a mutant 4IQ myoV in which the lever arms were shortened by 33% by the removal of two IQ domains (see Fig. 1). As expected, this mutant walks with a shorter step size of $\sim$24 nm (Purcell et al., 2002; Sakamoto et al., 2003) because of both a shorter powerstroke displacement and the structural constraints created by the linking of the two shorter lever arms. If the structure of the 6IQ myoV evolved to match the actin-helical structure for efficient intracellular cargo delivery, then shortening the effective span of the two lever arms would place constraints on the appropriate actin monomers for this mutant to step on. When characterized in the present study, the axial angles of the lever arms were no different than the normal 6IQ myoV, being 124° and 56° for the leading and trailing levers, respectively. Given the 10° resolution of the system, it would be difficult to resolve the small expected changes in axial angles based purely on geometric considerations associated with the shorter levers (Fig. 1). However, if the probes are predominantly on the first calmodulin that resides next to the head, one might expect the axial angle to be unchanged because the probe should provide an estimate of the angular swing of the powerstroke, which should be independent of the lever-arm length and determined only by the conformational changes within the head that generate the powerstroke during the hydrolytic cycle of the motor. More interestingly, the $\Delta\alpha$ for the 4IQ mutant was no longer near 0° the majority of the time, which would have been the case if the motor landed on the same relative actin monomer time after time. Rather, the motor had $\Delta\alpha$ values that were equally distributed between −35°, −1.4°, and +47°, suggesting that the 4IQ mutant leading head can visit multiple monomer positions and thus should no longer exhibit any bias in its walking path along the actin filament. This was confirmed by the actin filament twirling assay in which both left- and right-handed twirlers were observed. These data and that of the normal 6IQ motor suggest that myoV's walking path is based on structural determinants, not only those of the motor itself but rather in combination with the helical actin filament structure as well.

How do these structural studies provide insight to myoV's capacity to maneuver through the complexities

of the actin cytoskeleton during its delivery of intracellular cargo? Although the lever arms are assumed rigid, there must be sufficient flexibility in the molecule to allow the motor to explore the actin filament surface through its binding to various actin monomers within the actin filament. This variable binding requires that the lever of the leading head adopt a significant azimuthal angle. The most likely source of flexibility to accommodate this angular constraint is in the region of the motor at which the two lever arms converge and dimerize via a coiled-coil interaction of the two heavy chains (Fig. 1). This putative site of flexibility has been suggested to act as a universal joint that allows the 3-D diffusive search of the free head before its binding to actin (Dunn and Spudich, 2007) as well as explaining the ability of the motor to switch filaments at actin filament–actin filament intersection, even when this would require a large (>90°) turning angle (Ali et al., 2007). This inherent flexibility within the motor coupled with several potential binding sites along its actin track affords the motor the capacity to sidestep an intracellular obstacle (e.g., microtubule, organelle) that would limit its delivery of cargo. In addition to traveling along single-actin filaments, myoV can also wander along actin filament bundles (e.g., stress fibers, filopodial bundles), switching between parallel actin filaments within the bundle (Nagy et al., 2008). Once again, this wandering behavior reflects both the inherent flexibility of the motor as well as its ability to bind azimuthally to actin filaments, which would have to be the case when the motor straddles between two filaments in a bundle. Clearly, Mother Nature has designed an efficient system for cargo delivery by tuning the myoV structure to match the track upon which it travels. Although this present study focused on the myoV lever-arm domain, the strength of the polTIRF assay and its structural and temporal resolution offer the potential for simultaneous multiple domain labeling of the molecule with different color fluorescent probes so that a real-time 3-D image of the various domains and their conformational flexibility can be defined to fully appreciate the full repertoire of myoV's transport capacity.

A special thanks to Guy Kennedy of the Instrumentation and Model Facility at the University of Vermont for his artistic contributions to the figure.

This work was supported by funds from the National Institutes of Health (grants HL059408 and GM094229).

REFERENCES

Ali, M.Y., S. Uemura, K. Adachi, H. Itoh, K. Kinosita Jr., and S. Ishiwata. 2002. Myosin V is a left-handed spiral motor on the right-handed actin helix. *Nat. Struct. Biol.* 9:464–467. http://dx.doi.org/10.1038/nsb803

Ali, M.Y., E.B. Krementsova, G.G. Kennedy, R. Mahaffy, T.D. Pollard, K.M. Trybus, and D.M. Warshaw. 2007. Myosin Va maneuvers through actin intersections and diffuses along microtubules. *Proc. Natl. Acad. Sci. USA.* 104:4332–4336. http://dx.doi.org/10.1073/pnas.0611471104

Dunn, A.R., and J.A. Spudich. 2007. Dynamics of the unbound head during myosin V processive translocation. *Nat. Struct. Mol. Biol.* 14:246–248. http://dx.doi.org/10.1038/nsmb1206

Forkey, J.N., M.E. Quinlan, M.A. Shaw, J.E. Corrie, and Y.E. Goldman. 2003. Three-dimensional structural dynamics of myosin V by single-molecule fluorescence polarization. *Nature.* 422:399–404. http://dx.doi.org/10.1038/nature01529

Lewis, J.H., J.F. Beausang, H.L. Sweeney, and Y.E. Goldman. 2012. The azimuthal path of myosin V and its dependence on lever-arm length. *J. Gen. Physiol.* 139:101–120.

Nagy, S., B.L. Ricca, M.F. Norstrom, D.S. Courson, C.M. Brawley, P.A. Smithback, and R.S. Rock. 2008. A myosin motor that selects bundled actin for motility. *Proc. Natl. Acad. Sci. USA.* 105:9616–9620. http://dx.doi.org/10.1073/pnas.0802592105

Purcell, T.J., C. Morris, J.A. Spudich, and H.L. Sweeney. 2002. Role of the lever arm in the processive stepping of myosin V. *Proc. Natl. Acad. Sci. USA.* 99:14159–14164. http://dx.doi.org/10.1073/pnas.182539599

Sakamoto, T., F. Wang, S. Schmitz, Y. Xu, Q. Xu, J.E. Molloy, C. Veigel, and J.R. Sellers. 2003. Neck length and processivity of myosin V. *J. Biol. Chem.* 278:29201–29207. http://dx.doi.org/10.1074/jbc.M303662200

Veigel, C., F. Wang, M.L. Bartoo, J.R. Sellers, and J.E. Molloy. 2002. The gated gait of the processive molecular motor, myosin V. *Nat. Cell Biol.* 4:59–65. http://dx.doi.org/10.1038/ncb732

Walker, M.L., S.A. Burgess, J.R. Sellers, F. Wang, J.A. Hammer III, J. Trinick, and P.J. Knight. 2000. Two-headed binding of a processive myosin to F-actin. *Nature.* 405:804–807. http://dx.doi.org/10.1038/35015592

Warshaw, D.M., G.G. Kennedy, S.S. Work, E.B. Krementsova, S. Beck, and K.M. Trybus. 2005. Differential labeling of myosin V heads with quantum dots allows direct visualization of hand-over-hand processivity. *Biophys. J.* 88:L30–L32. http://dx.doi.org/10.1529/biophysj.105.061903